15 August 1995

OPTICS COMMUNICATIONS

ELSEVIER

Optics Communications 119 (1995) 246–255

Full length article

Semiconductor laser dynamics beyond the rate-equation approximation

Jun Yao [a], Govind P. Agrawal [a], Philippe Gallion [b], Charles M. Bowden [c]

[a] *The Institute of Optics, University of Rochester, Rochester, NY 14627, USA*

[b] *Department Communications, Ecole Nationale Superieure des Telecommunications, 46 rue Barrault, 75634 Paris Cedex 13, France*

[c] *Weapons Sciences Directorate, AMSMI-RD-WS-ST, U.S. Army Missile Command, Redstone Arsenal, AL 35898, USA*

Received 22 November 1994; revised version received 7 March 1995

Abstract

Starting from the density-matrix equations, we have obtained a new set of generalized macroscopic Maxwell–Bloch equations for semiconductor lasers which can be used to study ultrafast phenomena at femtosecond time scales where the conventional rate equations are no longer valid. The band-structure details are included in these Maxwell–Bloch equations through two parameters κ and ζ which can be determined numerically by using their definitions or obtained experimentally by fitting the measured data. In the limit of ultrafast intraband relaxation (the rate-equation approximation), these equations reduce to the conventional rate equations. As an illustration of the usefulness of the new Maxwell–Bloch equations we have obtained the analytic expressions for several important laser parameters such as the differential gain, the linewidth enhancement factor and the nonlinear gain coefficient, in terms of the parameters κ and ζ when the semiconductor laser is operating continuously (the cw operation). The results obtained from these analytic expressions agree with those obtained numerically from the density-matrix equations under steady-state conditions by integrating over the density of states.

1. Introduction

The dynamic response of semiconductor lasers is generally modelled through a set of rate equations [1] similar to those used for other solid-state lasers [2]. Although the standard rate equations have proved extremely useful [1], their use becomes questionable at femtosecond time scales since the gain medium cannot be assumed to respond instantaneously in that case. When the induced polarization cannot be eliminated adiabatically, the well-known quantities such as the optical gain and the refractive index cannot even be defined since one cannot describe the medium response in term of dielectric susceptibilities. It is then necessary to employ the density-matrix formalism [3–5]. Although this formalism is quite general and permits even the introduction of many-body effects [6], its use typically requires multiple integrations over the density of states, making it necessary to resort to extensive numerical computations.

Recently an approximate technique was developed to carry out the integration over the density of states analytically and obtain a set of macroscopic dynamic equations [7,8], which represent a generalization of the Maxwell–Bloch equations commonly used for homogeneously broadened two-level systems [9] to the case of semiconductors. These equations include the band-structure details through a single parameter s and should be useful for describing semiconductor laser dynamics once the parameter s has been evaluated for a specific laser structure. However, the calculation of s is not straightforward. In fact, the integration over the

SSDI 0030-4018(95)00245-6

band states may even diverge depending upon the form of density of states. In this paper, we present an alternative formulation of the density-matrix equations and obtain a modified set of macroscopic Maxwell–Bloch equations for semiconductor lasers. In this new set, band-structure information is included through two parameters, both of which can be complex in general. We solve these equations exactly at the steady state and obtain analytic expressions for the laser parameters such as the differential gain, linewidth enhancement factor, and the nonlinear gain parameter. These analytic expressions agree with the results obtained previously by using numerical integration over the band states.

2. Density-matrix equations

In the density-matrix approach [3–5], the system dynamics is described by the density-matrix operator ρ which satisfies the Liouville equation

$$i\hbar \frac{d\rho}{dt} = [H_0 - \mu \cdot \boldsymbol{E}, \rho] + \left(\frac{d\rho}{dt}\right)_{\text{relax}} + \left(\frac{d\rho}{dt}\right)_{\text{pump}}, \quad (1)$$

where H_0 is the unperturbed Hamiltonian, μ is the dipole-moment, $\boldsymbol{E}$ is the electric field associated with the electromagnetic radiation, and the last two terms incorporate the effects of relaxation and pumping phenomenologically. The induced polarization $\boldsymbol{P}$ is obtained from

$$\boldsymbol{P}(t) = \frac{1}{V} \sum_k \mu_{21} \rho_{21}(t) + \text{c.c.}, \quad (2)$$

where V is the volume, c.c. stands for complex conjugate, $\rho_{21} = \langle 1|\rho|2\rangle$, and $\mu_{21} = \langle 2|\mu|1\rangle$. The states $|1\rangle$ and $|2\rangle$ correspond to electronic Bloch states of momentum $\hbar \boldsymbol{k}$ in the conduction and valence bands respectively. The sum in Eq. (2) is over all the electronic states of different momenta. By defining the matrix elements $\rho_{ij} = \langle i|\rho|j\rangle$ for $i, j = 1$ and 2, and using Eq. (1), the density-matrix equations can be written as [3–5]:

$$\frac{d\rho_{11}}{dt} = \Lambda_e - \frac{\rho_{11} - \bar{\rho}_{11}}{\tau_c} - \frac{\rho_{11} - \rho_{11}^{th}}{\tau_e} + \frac{\mu}{i\hbar}(\rho_{12} - \rho_{21})\boldsymbol{E}(t), \quad (3)$$

$$\frac{d\rho_{22}}{dt} = -\Lambda_h - \frac{\rho_{22} - \bar{\rho}_{22}}{\tau_v} - \frac{\rho_{22} - \rho_{22}^{th}}{\tau_e} - \frac{\mu}{i\hbar}(\rho_{12} - \rho_{21})\boldsymbol{E}(t), \quad (4)$$

$$\frac{d\rho_{12}}{dt} = -(i\omega + 1/\tau_{in})\rho_{12} + \frac{\mu}{i\hbar}(\rho_{11} - \rho_{22})\boldsymbol{E}(t), \quad (5)$$

where $\mu = \hat{\boldsymbol{e}} \cdot \langle 2|\mu|1\rangle$ is the transition dipole moment with $\hat{\boldsymbol{e}}$ being the polarization unit vector of the electric field, ω is the transition frequency, τ_e is the interband carrier relaxation time ($\tau_e \sim 1$ ns), τ_c and τ_v are the intraband relaxation times (~ 0.1 ps) for conduction and valence band, and τ_{in} is the dipole relaxation time (< 0.1 ps) due to intraband scattering. ρ^{th} and $\bar{\rho}$ are the density matrices at thermal and quasi-equilibrium respectively. The pumping rates Λ_e and Λ_h present the electron and hole injection rates and are related to the injected current I as

$$\Lambda_e = \frac{I}{q} \frac{\bar{\rho}_{11}}{\sum_k \bar{\rho}_{11}}, \qquad \Lambda_h = \frac{I}{q} \frac{1 - \bar{\rho}_{22}}{\sum_k [1 - \bar{\rho}_{22}]}. \quad (6)$$

It should be stressed that the use of phenomenological intraband relaxation times and a simplified injection-rate model makes Eqs. (3)–(5) valid only on time scales longer than the intraband relaxation time (> 0.1 ps). For pulses shorter than 100 fs it becomes necessary to consider finer details of carrier injection and relaxation process.

Eqs. (3)–(5) are microscopic Bloch equations and can be easily generalized to include the many-body effects [6]. They can be simplified considerably by making the rotating-wave approximation which amounts to assuming that one is interested in time scales much longer than the optical cycle associated with the laser carrier frequency ω_0. By introducing the slowly varying quantities E and p through

$$\boldsymbol{E}(t) = \hat{\boldsymbol{e}} \tfrac{1}{2}[E \exp(-i\omega_0 t) + \text{c.c.}],$$
$$\rho_{12} = p \exp(-i\omega_0 t), \quad (7)$$

and neglecting the rapidly oscillating terms at the frequency $2\omega_0$, the microscopic Bloch equations can be written as

$$\frac{dn_c}{dt} = \Lambda_c - \frac{n_c - \bar{n}_c}{\tau_c} - \frac{n_c - n_c^{th}}{\tau_c} + \frac{\mu}{2i\hbar}(E^*p - Ep^*), \quad (8)$$

$$\frac{dn_h}{dt} = \Lambda_h - \frac{n_h - \bar{n}_h}{\tau_v} - \frac{n_h - n_h^{th}}{\tau_c} + \frac{\mu}{2i\hbar}(E^*p - Ep^*), \quad (9)$$

$$\frac{dp}{dt} = -\frac{1+i\delta}{\tau_{in}}p + \frac{\mu E}{2i\hbar}(n_e + n_h - 1), \quad (10)$$

where we have introduced $n_e = \rho_{11}$ and $n_h = 1 - \rho_{22}$ as the occupation probabilities for electrons and holes respectively. The detuning parameter δ is defined as

$$\delta = (\omega - \omega_0)\tau_{in}. \quad (11)$$

Integration over the band states is equivalent to integrating over δ.

3. Macroscopic Maxwell–Bloch equations

The use of microscopic Bloch equations requires an integration over the band states in order to evaluate the total induced polarization given by (2). In this section, we follow an approximate technique that permits us to perform this integration analytically. The macroscopic variables we want to use are the injected carrier density N related to n_e and n_h as

$$N = \frac{1}{V}\sum_k n_e = \frac{1}{V}\sum_k n_h, \quad (12)$$

and the slowly varying polarization P defined in a manner similar to Eq. (7) by using

$$\boldsymbol{P} = \tfrac{1}{2}\hat{\boldsymbol{e}}[P\exp(-i\omega_0 t) + \text{c.c.}]. \quad (13)$$

By using Eqs. (2), (7) and (13), P is related to p as

$$P = 2\mu\frac{1}{V}\sum_k p. \quad (14)$$

If the sum over $\boldsymbol{k}$ is replaced by an integration over the density of states $D(\boldsymbol{E})$, N and P are defined as

$$N = \int_{E_g}^{\infty} n_e(\boldsymbol{E}')\, D(\boldsymbol{E}')\, d\boldsymbol{E}' = \int_{-\delta_g}^{\infty} n_e(\delta)\, D(\delta)\, d\delta = \langle n_e \rangle, \quad (15a)$$

$$P = 2\mu\int_{E_g}^{\infty} p(\boldsymbol{E}')\, D(\boldsymbol{E}')\, d\boldsymbol{E}' = 2\mu\int_{-\delta_g}^{\infty} p(\delta)\, D(\delta)\, d\delta = 2\mu\langle p \rangle, \quad (15b)$$

where the integration over band energies was converted to integration over the detuning by using Eq. (11) with $\boldsymbol{E}' = \hbar\omega$. The lower limit δ_g is then given by $\delta_g = (\omega_0 - E_g/\hbar)\tau_{in}$, where E_g is the band gap energy. In Eq. (15) angular brackets denote macroscopic quantities obtained after integration over the band states.

The carrier density equation is readily obtained by multiplying Eq. (8) or (9) by $D(\delta)$ and performing the integration. The result is:

$$\frac{dN}{dt} = \frac{I}{qV} - \frac{N}{\tau_e} + \frac{1}{2\hbar}\,\text{Im}(E^*P), \quad (16)$$

where the term containing τ_c or τ_v does not appear since the total carrier density remains unaffected by intraband relaxation of individual electrons. We have also assumed that carrier density is negligible in thermal equilibrium.

When the same process is repeated for the induced polarization P, it is not possible to get a closed form for dP/dt because of the presence of the term $\langle \delta p \rangle$. This is a well-known feature in the literature on inhomogeneously broadened two-level systems [10]. If we define a new dynamic variable $\langle \delta p \rangle$, we obtain a term containing $\langle \delta^2 p \rangle$ and so on, resulting in an infinite hierarchy of coupled equations. The only solution is to solve the problem approximately by truncating the infinite hierarchy. In a recent paper [7], the hierarchy was truncated at the term containing $\langle \delta^2 p \rangle$. The band-structure details were then incorporated through a single parameter s defined as $s^2 = \langle \delta^2 p \rangle / \langle p \rangle$. However, when this parameter s is evaluated by performing the integration over δ, the integral

$$\langle \delta^2 p \rangle = \int_{-\delta_g}^{\infty} \delta^2 p(\delta)\, D(\delta)\, \mathrm{d}\delta , \tag{17}$$

diverges. In this paper, we adopt an alternative approach. Specifically, we divide Eq. (10) by $1+\mathrm{i}\delta$ before integrating over the band states, and introduce two parameters κ and ζ as

$$\left\langle \frac{n_e + n_h - 1}{1+\mathrm{i}\delta} \right\rangle = \kappa N , \tag{18}$$

$$\left\langle \frac{p}{1+\mathrm{i}\delta} \right\rangle = \frac{P}{2\mu\zeta} . \tag{19}$$

In terms of the parameters κ and ζ, the induced polarization is given by

$$\frac{\mathrm{d}P}{\mathrm{d}t} = -\frac{\zeta}{\tau_{in}} P + \frac{\zeta \kappa \mu^2}{\mathrm{i}\hbar} EN . \tag{20}$$

Eqs. (16) and (20) are the macroscopic Bloch equations. In the evaluation of both equations, the dependence of dipole moment on the transition energy has been neglected. Their approximate nature results from Eqs. (18) and (19). This approximation can be partially justified by noting that the main contribution to the integral comes for values of δ such that $\delta \ll 1$. Thus, we expect the approximation to hold reasonably well in the vicinity of the gain peak.

The usefulness of Eq. (20) hinges on whether the parameters κ and ζ are constants or depend on the carrier density N and the mode intensity $|E|^2$. It will be seen in the next section that these parameters are nearly independent of the mode intensity at typical operating powers well below the intraband saturation intensity. However, they depend on the carrier density N. The dependence of κ on N is quite weak in the above-threshold regime and it can be treated approximately as constant. In contrast, the dependence of ζ on N cannot be ignored. We discuss in Section 4 how this dependence can be included in Eq. (20).

The field equation is obtained by considering the Maxwell wave equation [3]

$$\nabla^2 \boldsymbol{E} - \frac{\sigma}{\epsilon_0 c^2}\frac{\partial \boldsymbol{E}}{\partial t} - \frac{1}{c^2}\frac{\partial^2 \boldsymbol{E}}{\partial t^2} = \frac{1}{\epsilon_0 c^2}\frac{\partial^2 \boldsymbol{P}}{\partial t^2} . \tag{21}$$

In the case of semiconductor lasers the conductivity σ can be used to include cavity losses. By using Eqs. (7) and (13), and adopting a mean-field approach for the intracavity field $E(t)$, Eq. (21) in the slowly varying envelope approximation becomes

$$\frac{\mathrm{d}E}{\mathrm{d}t} = \frac{\mathrm{i}\omega_0}{2nn_g\epsilon_0} P - \frac{E}{2\tau_p} , \tag{22}$$

where the photon lifetime τ_p takes into account cavity losses. The dynamics of semiconductor lasers is thus governed by a set of three coupled equations, Eqs. (16), (20) and (22), similar to Maxwell–Bloch equations obtained for a two-level atomic system. The effects of band structure appear through two parameters κ and ζ. These macroscopic equations do not include the effects of carrier heating. However, as discussed in the Appendix, carrier heating can be included in a straightforward manner.

4. Determination of the parameters κ and ζ

The parameters κ and ζ depend on the band-structure details as indicated by Eqs. (18) and (19). Physically from Eq. (20), ζ governs modification of the intraband relaxation time for the macroscopic polarization P. Since ζ is generally complex, such a modification not only alters the damping time of polarization but also introduces an effective detuning. By introducing $\zeta = \zeta_r + \mathrm{i}\zeta_i$, we can identify ζ_r/τ_{in} and ζ_i/τ_{in} as the effective damping rate and detuning for the macroscopic polarization. By contrast, the κ parameter governs changes in the medium susceptibility resulting from integrating over the band states in semiconductors and affects both the gain and the refractive index.

Exact determination of κ and ζ is not easy and, in fact, is not even possible if we note from Eqs. (18) and (19) that they can be calculated only if the time dependence of the microscopic variables n_e, n_h, and p is known. However, one expects them to vary slowly with time since the macroscopic variables N and P take into account the time dependence in Eqs. (18) and (19). For a first approximation, we can use the steady-state values of p, n_e and n_h, denoted by p^s, n_e^s and n_h^s respectively, to calculate κ and ζ. The steady-state solution of Eqs. (8)–(10) is the same as that of a two-level atomic system [9] and is given by

$$n_c^s = \bar{n}_e - \frac{\mu^2 \tau_c \tau_{in} |E|^2 (\bar{n}_e + \bar{n}_h - 1)}{2\hbar^2 (1 + \delta^2 + |E|^2/I_s)}, \quad (23)$$

$$n_h^s = \bar{n}_h - \frac{\mu^2 \tau_v \tau_{in} |E|^2 (\bar{n}_e + \bar{n}_h - 1)}{2\hbar^2 (1 + \delta^2 + |E|^2/I_s)}, \quad (24)$$

$$p^s = \frac{\mu E \tau_{in}}{2i\hbar(1 + i\delta)} \frac{(\bar{n}_e + \bar{n}_h - 1)(1 + \delta^2)}{1 + \delta^2 + |E|^2/I_s}, \quad (25)$$

where $I_s = \hbar^2 [\mu^2 (\tau_c + \tau_v) \tau_{in}]^{-1}$ is the intraband saturation intensity, and τ_c and τ_v are assumed to be much smaller than τ_c. By using Eqs. (18), (19) and (23)–(25), we can determine the values of κ and ζ for a specific laser structure by performing the integration numerically. In the calculation of κ_i, we encounter the following divergent integral

$$\kappa_i = -\frac{1}{N} \int_{-\delta_g}^{\infty} \frac{D(\delta)\,(n_e + n_h - 1)\,\delta}{1 + \delta^2} \, d\delta. \quad (26)$$

This is not surprising since κ_i is related to the refractive index whose evaluation has always been found to encounter the divergence problem within the density-matrix formalism [11]. Therefore, we adopt an approach similar to that used in previous work. We expand n_e and n_h in a Taylor series with respect to the injected carrier density N and approximate κ_i by

$$\kappa_i = -\int_{-\delta_g}^{\infty} \frac{D(\delta)\,(dn_e/dN + dn_h/dN)\,\delta}{1 + \delta^2} \, d\delta. \quad (27)$$

The contribution to κ_i under thermal equilibrium conditions (occurring in the absence of carrier injection) is ignored here by assuming that it can be included in the definition of the background refractive index (discussed in the next section).

In the following we consider bulk and quantum-well lasers operating near 1.5 μm to show how κ and ζ vary with various laser parameters, such as the operating wavelength, the carrier density and the laser intensity. Our model structures are an $In_{0.53}Ga_{0.47}As/InP$ bulk laser and an $In_{0.53}Ga_{0.47}As/In_{0.72}Ga_{0.28}As_{0.6}P_{0.4}/InP$ separated confinement quantum-well (QW) laser with well thickness equal to 10 nm. The values of material parameters used in numerical calculations are given in Table 1.

The wavelength dependence of κ at a carrier density $N = 3 \times 10^{18}$ cm^{-3} is shown in Fig. 1 for the case in which gain and index nonlinearities are ignored by assuming $|E|^2/I_s \ll 1$. The real and imaginary parts are shown separately and compared for bulk and QW lasers. As discussed in the next section, the parameters κ_r and κ_i are in fact linearly related to the optical gain and carrier-induced refractive index respectively. For this reason, the curves in Fig. 1a mimic the gain curves expected for bulk and QW lasers. For example, the maximum value of κ_r is larger for QW lasers since QW lasers exhibit larger gain at a given carrier density. As seen in Fig. 1b, κ_i is negative since carrier injection reduces the refractive index. The absolute value of κ_i is smaller in QW lasers than in bulk laser since QW lasers generally have smaller index changes for a given carrier density.

Table 1
Material parameters used in numerical calculations.

Material parameters	Values
Temperature	300 K
Effective mass of electrons	0.041 m_0
Effective mass of holes	0.4235m_0
Average refractive index	3.4
Group index	4.0
Band gap	0.75 eV
Spin-orbit splitting	0.33 eV
Intraband relaxation time for dipole moment	0.07 ps
Intraband relaxation time for electrons	0.1 ps
Intraband relaxation time for holes	0.2 ps

We have also investigated the carrier-density dependence of κ and ζ for the wavelengths at which the gain is maximum. The results are shown in Figs. 2 and 3. One can see from Fig. 2a that for both structures, with increasing carrier densities, κ_r increases with N at low carrier densities but eventually saturates and begins to decrease at high carrier densities. Because the refractive index decreases with carrier density, the absolute value of κ_i should decrease with N for both structures, as seen in Fig. 2b. From Fig. 3a, we note that the value of ζ_r increases with carrier density and is normally larger than 1 in the usual carrier density region for both structures. This feature indicates that macroscopic polarization decays more rapidly compared with the microscopic dipole moments associated with individual transitions in bulk and QW lasers. Note also that at a given carrier density ζ_r is larger for QW lasers com-

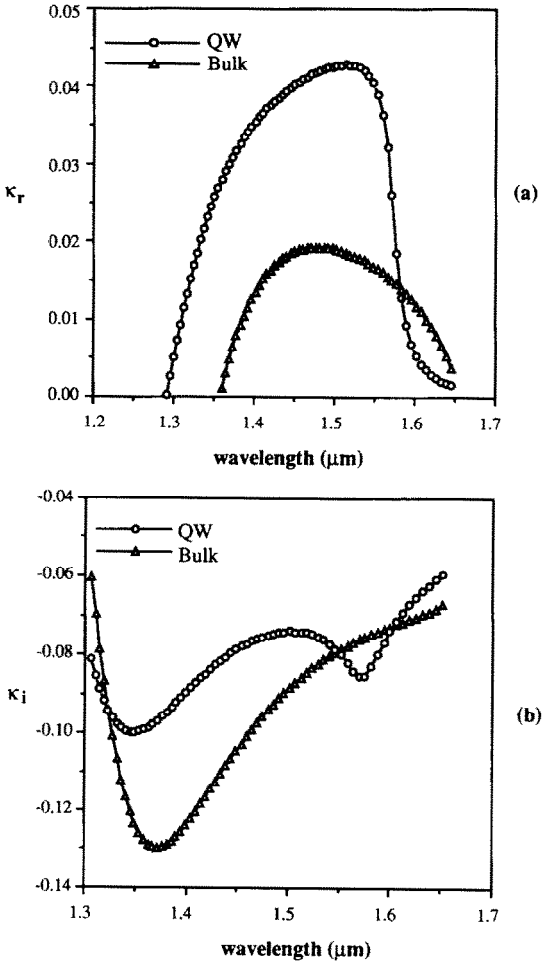

Fig. 1. The real (a) and imaginary (b) parts of κ at a carrier density of 3×10^{18} cm^{-3} as a function of wavelength for an $In_{0.53}Ga_{0.47}As/InP$ bulk laser and an $In_{0.53}Ga_{0.47}As/In_{0.72}Ga_{0.28}As_{0.6}P_{0.4}/InP$ quantum well (QW) laser with well thickness equal to 10 nm. Other parameters are given in Table 1.

pared with bulk lasers, resulting in a more rapid decay of macroscopic polarization. This is consistent with Fig. 1a which shows that QW lasers have a wider gain spectrum. It is well known [2] that the gain bandwidth is inversely related to the damping time of macroscopic polarization. In the Fig. 3b, we can observe that the absolute value of ζ_i is smaller in QW lasers than in bulk lasers. This is quite understandable in view of the step-like nature of the density of states associated with the QW lasers. Since most transitions correspond to the lowest QW states, effective detuning is expected to be quite small. The change of effective detuning with carrier density is very small in the QW laser while in the bulk laser it increases considerably with carrier density.

The parameter κ depends on the laser intensity in view of the steady-state solution given by Eqs. (23)–(25). The dependence of κ_r on the intensity is shown in the Fig. 4 for both QW and bulk lasers. Dashed lines show that this dependence fits quite well an expression of the form $\kappa_r = \kappa_{r0}/\sqrt{1+|E|^2/I_s}$ for both structures. It is important to note that our analysis includes gain and index nonlinearities automatically.

As seen in the Figs. 2 and 3, the parameters κ and ζ appearing in Eq. (20) vary with the carrier density N. The dependence of κ on N is quite weak for $N>$

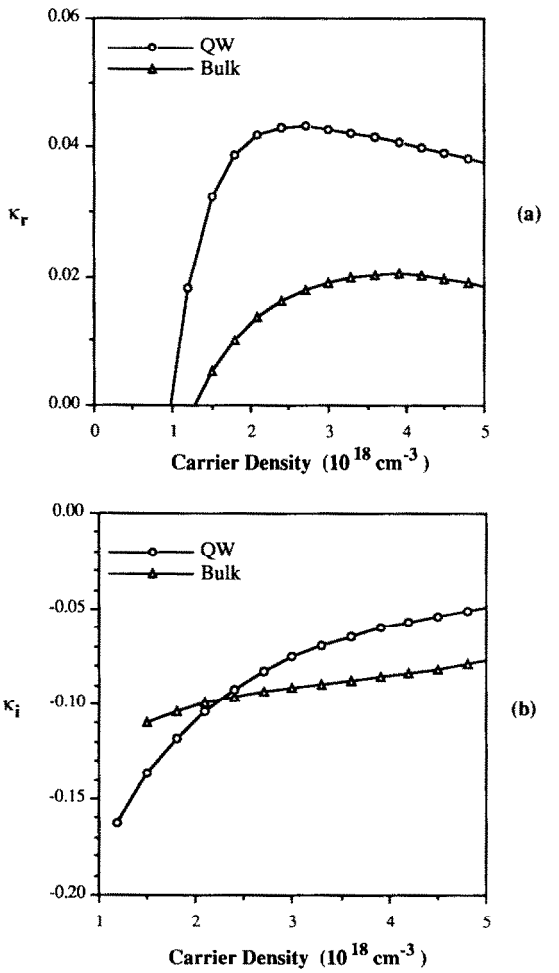

Fig. 2. The real (a) and imaginary (b) parts of κ as a function of carrier density for the bulk and QW lasers operating at the gain peak. Other parameters are the same as in Fig. 1.

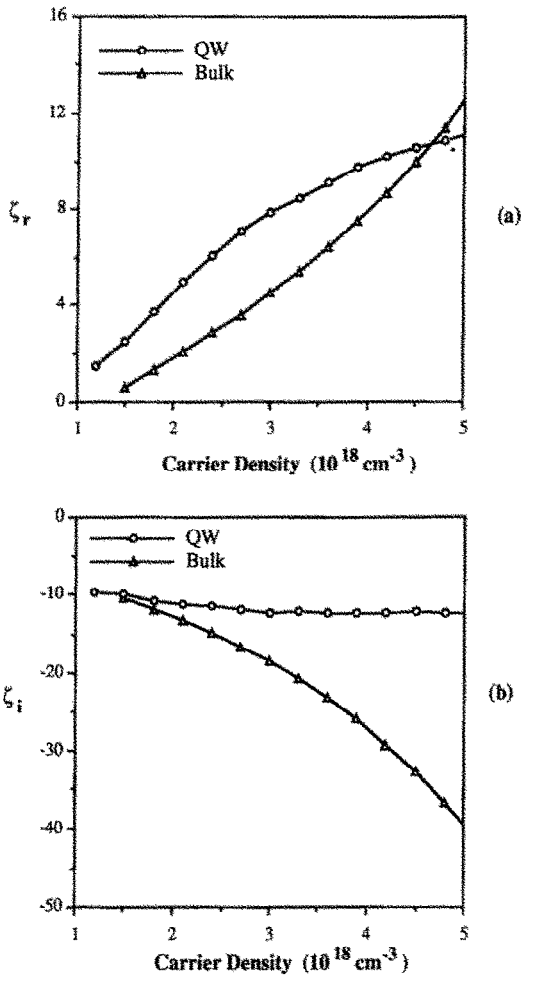

Fig. 3. The real (a) and imaginary (b) parts of ζ as a function of carrier density for the bulk and QW lasers operating at the gain peak.

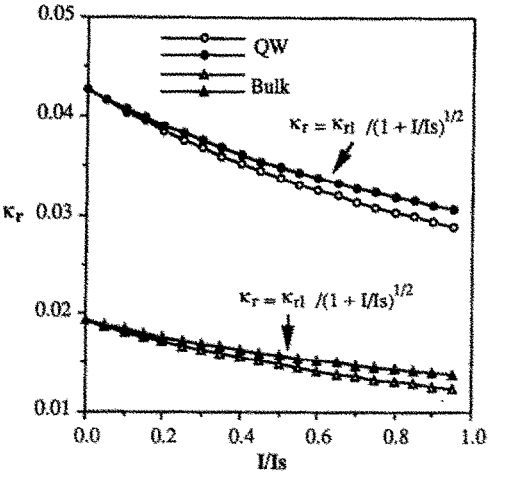

Fig. 4. Variation of κ_r with normalized intensity for the bulk and QW lasers operating at the gain peak with a carrier density of 3×10^{18} cm^{-3}.

2×10^{18} cm^{-3}. In most semiconductor lasers N exceeds 2×10^{18} cm^{-3} before the laser threshold is reached. Moreover, N varies relative little ($\sim1\%$) even when the laser intensity is modulated as long as the laser is not driven too much below threshold. For this reason, the parameter κ can be treated as approximately constant in Eq. (20). In contrast, the dependence of ζ on N is quite strong and cannot be ignored. This is not unexpected since the relaxation time of induced polarization should depend on the number of electrons present in the conduction band. A simple way to include this dependence of ζ on N in Eq. (20) is to assume that ζ varies linearly with N. The assumption is quite justified from Fig. 3 over the limited range over which N is likely to vary in most semiconductor lasers. It is similar to the usual rate-equation approximation that the peak gain of semiconductor lasers varies linearly with N. Specifically, ζ in Eq. (20) is replaced by $\zeta = bN - c$, where b and c are complex and their real and imaginary parts are obtained by fitting a straight line to the curve shown in Fig. 3 in the vicinity of N_{th}, the threshold value of the carrier density under steady-state operation. For $N_{th} = 3\times10^{18}$ cm^{-3}, $b = (2.8 - 7.4\mathrm{i})\times10^{-18}$ cm^3, $c = 2.6 + 2\mathrm{i}$ for bulk lasers whereas $b = 2.1\times10^{-18}$ cm^3 and $c = 12.2\mathrm{i}$ for QW lasers.

5. Rate-equation approximation

The new set of Maxwell–Bloch equations should yield the usual rate equations when P is adiabatically eliminated by assuming that the medium response is very rapid. By setting $dP/dt = 0$ in Eq. (20), we obtain

$$P = \frac{\mu^2 \tau_{in} \kappa N}{i\hbar} E. \qquad (28$$

Since P is proportional to the optical field E, we can introduce the concept of medium susceptibility using the definition $P = \epsilon_0 \chi E$, and ϵ_0 is the vacuum permittivity. Eq. (28) then provides us with the following expression for the susceptibility χ

$$\chi = \frac{\mu^2 \tau_{in} \kappa N}{i\hbar\epsilon_0}.$$

By using the dielectric constant $\epsilon = 1 + \chi = (n + \Delta n)^2 - ignc/\omega_0$, where n is the background refractive index, the optical gain g, the carrier-induced refractive index Δn, and the linewidth enhancement factor α are given by

$$g = -\frac{\omega_0}{cn}\,\mathrm{Im}(\chi) = \frac{\mu^2 \tau_{in}\omega_0 N}{\epsilon_0 cn\hbar}\,\kappa_r \tag{30}$$

$$\Delta n = \frac{1}{2n}\,\mathrm{Re}(\chi) = \frac{\mu^2 \tau_{in} N}{2\epsilon_0 n\hbar}\,\kappa_i\,, \tag{31}$$

$$\alpha = \frac{\mathrm{Re}(\chi)}{\mathrm{Im}(\chi)} = -\frac{\kappa_i}{\kappa_r}\,. \tag{32}$$

By substituting the Eq. (28) into Eq. (16), we recover the conventional rate equation for carrier density

$$\frac{dN}{dt} = \frac{I}{qV} - \frac{N}{\tau_c} - v_g g S\,, \tag{33}$$

where $S = \epsilon_0 n n_g |E|^2/2\hbar\omega_0$ is the photon density, $v_g = c/n_g$ is the group velocity, and n_g is the group index.

From Eq. (30), we can obtain an analytic expression for the differential gain in terms of κ_r. The result is

$$\frac{dg}{dN} = \frac{\mu^2 \omega_0 \tau_{in}}{\epsilon_0 cn\hbar}\left(\kappa_r + \frac{N}{\omega_0}\frac{d(\omega_0 \kappa_r)}{dN}\right). \tag{34}$$

Normally for low carrier densities, the second term in the bracket of Eq. (34) is smaller than κ_r. Therefore, as a first approximation, we can neglect the second term and obtain the following approximate analytic expression for the differential gain

$$\frac{dg}{dN} \approx \frac{\mu^2 \omega_0 \tau_{in}}{\epsilon_0 cn\hbar}\,\kappa_r\,. \tag{35}$$

Since κ_r and κ_i can be calculated for any laser structure as discussed in Section 4, Eqs. (30)–(32), and (34) provide us with the analytic expressions for the gain, refractive index, the linewidth enhancement factor and differential gain in terms of a single parameter κ. We have calculated g, Δn, and α by using these equations and have verified that their values are exactly the same as those obtained directly from the density-matrix equations when the dependence of dipole moment on the transition energy is neglected. The differential gain for a carrier density of 3×10^{18} cm^{-3} obtained by using the approximate expression Eq. (35) is 2.44×10^{-16} cm^2 and 8.32×10^{-16} cm^2 for our model bulk and QW lasers operating at the gain peak, while its exact value is 4.13×10^{-16} cm^2 and 7.26×10^{-16} cm^2 respectively. We find reasonable agreement between the values of differential gain obtained from the approximate and the exact calculations for both structures. However, the accord is better in the QW laser because of the larger value of κ_r in this laser. In general, one must use Eq. (34) for calculating the differential gain.

The carrier-density dependence of maximum gain, refractive index and linewidth enhancement factor can be obtained by using Eqs. (30)–(32). Our model predicts gain saturation for high carrier densities in the QW laser and the quasi-linear increase of the maximum gain carrier density for the bulk laser. These well-known features have been obtained from direct evaluation of the density-matrix equations and confirmed by experimental observations. As a further usefulness of our approach, Fig. 5 plots the linewidth enhancement factor α as a function of carrier density for bulk an QW lasers operating at the gain peak. Normally, α is treated as independent of carrier density N. As seen in Fig. 5, this is not generally the case. The linewidth enhancement factor decreases with carrier density for both structures and, as one should expect, the value of α is smaller for the QW laser compared with bulk laser.

From Eq. (30), we note that the intensity dependence of κ_r reflects the nonlinear nature of the optical

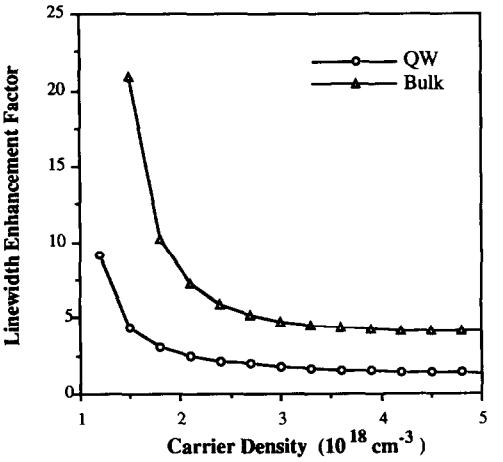

Fig. 5. Dependence of linewidth enhancement factor on carrier density for the bulk and QW lasers operating at the gain peak.

gain. Numerical results shown in Fig. 4 indicate the intensity dependence of κ_r can be well approximated by $\kappa_r = \kappa_{r0}/\sqrt{1+|E|^2/I_s}$; the gain g then also varies as $g = g_l/\sqrt{1+|E|^2/I_s}$. This form of nonlinear gain was predicted analytically by Agrawal [5] in 1988 by evaluating the integration over the band states approximately. For $|E|^2/I_s \ll 1$, $g \approx g_l(1-\epsilon S)$, where ϵ is nonlinear gain coefficient, defined as

$$\epsilon = \frac{\omega_0 \mu^2 (\tau_c + \tau_v)\tau_{in}}{\hbar \epsilon_0 n n_g}. \tag{36}$$

Thus our analysis provides an analytic expression for the nonlinear gain coefficient ϵ. The value of ϵ for a carrier density of 3×10^{18} cm^{-3} obtained by using Eq. (36) is 3.2×10^{-23} m^3 and 4.9×10^{-23} m^3 for our model bulk and QW lasers operating at peak gain. The higher gain nonlinearity in QW lasers mainly comes from the higher value of dipole moment. Note that Eq. (36) provides only the contribution of spectral hole-burning to the nonlinear gain. The contribution of carrier heating can be included by following the details given in the Appendix.

6. Conclusions

In this paper, we have obtained a new set of generalized macroscopic Maxwell–Bloch equations for semiconductor lasers which can be used to study ultrafast phenomena at femtosecond time scales where the conventional rate equations normally used to study semiconductor laser dynamics are no longer valid. This set of Maxwell–Bloch equations is an alternative approximate form of microscopic density-matrix equations. In spite of its approximate nature, it should prove useful for studying the ultrafast optical phenomena in semiconductor lasers because one does not have to perform multiple integrations over the band states as in the case of using the density-matrix equations. The band-structure details appear in these Maxwell–Bloch equations through two parameters κ and ζ which can be determined either numerically by using their definitions or by fitting experimental results. In the rate equation approximation, the macroscopic Maxwell–Bloch equations reduce to the conventional rate equations. Furthermore, they provide us with the analytic expressions for the gain, differential gain, carrier-induced refractive index change, the linewidth enhancement factor and nonlinear gain coefficient in terms of a single parameter κ. The results obtained from these analytic expression agree with those obtained numerically from the density-matrix equations under steady state condition.

It is important to emphasize that Eq. (20) for macroscopic polarization describes laser dynamics only approximately, and the results are not expected to be as accurate as those obtained using microscopic semiconductor Bloch equations incorporating the many-body effects [6]. It should nonetheless be useful as it extents the validity of conventional rate equations to femtosecond time scales as short as ~ 100 fs and can be used to obtain qualitative trends and dependence on various device parameters in a simple way. The establishment of the validity of our Maxwell–Bloch equations under dynamical conditions requires the solution of a time-dependent problem such as the amplification of ultrashort pulses in semiconductor laser amplifiers. However, such a solution is of little use unless it is compared with the solution of microscopic semiconductor Bloch equations and/or with the experimental data. Further work is necessary to establish the conditions under which the macroscopic equations of this paper can be used in practice. We have recently succeeded in incorporating the many-body effects in the macroscopic Maxwell–Bloch equations, and the results appear elsewhere [12].

Acknowledgements

The research is partially supported by NATO, the U.S. Army Research Office, and the NASA-Ames Research Center. Technical discussions with Peter Goorjian are gratefully acknowledged.

Appendix: inclusion of carrier heating

The macroscopic Maxwell–Bloch equations obtained in Section 3 include the nonlinear-gain reduction occurring because of spectral hole-burning. In fact, they were used in Section 5 to obtain an analytic expression for the nonlinear-gain parameter ϵ. However, these equations do not include the effects of carrier heating. Since, the phenomenon of carrier heating plays an important role in governing the ultrafast dynamics of semiconductor laser amplifiers [13–15] and occurs on

a time scale ~600 fs, it is important to discuss how carrier heating can be incorporated in the formalism used in this paper.

A simple approach consists of considering the temporal evolution of the energy densities U_e and U_h of electrons in the conduction band and of holes in the valence band [15]. These energy densities are defined as

$$U_e = \int_{E_g}^{\infty} E' n_e(E')\, D(E')\, D(E')\, dE' , \qquad (A1)$$

$$U_h = \int_{E_g}^{\infty} E' n_h(E')\, D(E')\, dE' . \qquad (A2)$$

In terms of the detuning parameter δ (see Eq. (11)), U_e and U_h can be related to the macroscopic quantities $\langle \delta n_e \rangle$ and $\langle \delta n_h \rangle$ respectively. At this point, one can follow the analysis of Ref. [15] to derive the macroscopic rate equations for U_e and U_h, which should be solved together with the macroscopic Maxwell–Bloch equations obtained in Section 3.

References

[1] G.P. Agrawal and N.K. Dutta, Semiconductor Lasers, 2nd. Ed. (Van Nostrand Reinhold, New York, 1993).
[2] A.E. Siegman, Lasers (University Science Books, Mill Valley, California, 1986).
[3] G.P. Agrawal, IEEE J. Quantum Electron. QE-23 (1987) 860.
[4] M. Yamada, J. Appl. Phys. 66 (1989) 81.
[5] G.P. Agrawal, J. Appl. Phys. 63 (1988) 1232.
[6] M. Linderberg and S.W. Koch, Phys. Rev. B 38 (1988) 3342.
[7] C.M. Bowden and G.P. Agrawal, Optics Comm. 100 (1993) 147.
[8] G.P. Agrawal and C.M. Bowden, IEEE Photon. Technol. Lett. 5 (1993) 640.
[9] L. Allen and J.H. Eberly, Optical Resonance and Two-level Atoms (Wiley, New York, 1975).
[10] R. Graham and Y. Cho, Optics Comm. 47 (1983) 52.
[11] A. Sugimura, E. Patzak, and P. Meissner, J. Phys. D: Appl. Phys. 19 (1986) 7.
[12] C.M. Bowden and G.P. Agrawal, Phys. Rev. A 51 (1995) 4132.
[13] K.L. Hall, J. Mark, E.P. Ippen and G. Eisenstein, Appl. Phys. Lett. 56 (1990) 1740.
[14] B.N. Gomatam and A.P. De Fonzo, IEEE J. Quantum Electron. 26 (1990) 1689.
[15] M. Willatzen, A. Uskov, J. Mork, H. Olesen, B. Tromborg and A.P. Jauho, IEEE 3 (1991) 606.